Наносистеми, наноматеріали, нанотехнології
Nanosistemi, Nanomateriali, Nanotehnologii
2026, т. 24, № 1, сс. 1–16
https://doi.org/10.15407/nnn.24.01.0001

PACS numbers: 71.10.Pm, 71.45.Lr, 73.22.Lp, 73.43.Lp, 75.30.Fv, 75.47.Lx

Formation of Bosons in $SmMnO_{3+}$ as 1*D* Charge/Spin Density Waves Caused by Confinement of Spinon Pairs in a System of AFM Spin Chains; Step-Like Quantum Hall Effect for Massless Dirac Fermions

F. M. Bukhanko

Donetsk Institute for Physics and Engineering Named after O. O. Galkin, N.A.S. of Ukraine,
46 Nauky Ave.,
UA-03028 Kyiv, Ukraine

As shown, the appearance of two unusual peak features of isotherms 1 and 2 of the magnetization reversal of $SmMnO_{3+\delta}$ near zero magnetic field is a natural consequence of the spin–charge separation characteristic of the previously well-studied theoretically one-dimensional Mott insulator in the state of a quantum Luttinger liquid. Attention is drawn to the difference between the two peak features of isotherms 1 and 2 of the magnetization reversal near $H = 0$ Oe, which depends on the direction of growth of the external magnetic-field strength. We believe that such behaviour of magnetization in the low-temperature region is caused by the fact that the transverse component of the external magnetic field closes the spinon gap Δ_s in $SmMnO_{3+\delta}$. A characteristic feature of this state is the spatial separation of charge and spin excitations. According to these studies, even a weak increase in the transverse component of the external magnetic field can lead to further confinement of spinon pairs, which is accompanied by the appearance of gapless modes of natural longitudinal oscillations of the spin chain system. We assume that the step-like features of field dependences of magnetization of $SmMnO_{3+\delta}$ at temperature $T = 0.6$ K are similar to characteristics of step-like quantum Hall effect for massless Dirac fermions in graphene.

Показано, що поява двох незвичайних пікових особливостей ізотерм 1 і 2 перемагнетування $SmMnO_{3+\delta}$ поблизу нульового магнетного поля є природнім наслідком характеристики розділення спін-зарядів раніше добре вивченого теоретично одновимірного Моттового ізолятора у стані квантової Латтинжерової рідини. Звертається увага на ріжницю між двома піковими особливостями ізотерм 1 і 2 перемагнетування поблизу $H = 0$ Е, яка залежить від напрямку зростання напружености зовнішнього магнетного поля. Ми вважаємо, що таку поведінку намагнетованости в області низьких температур зумовлено тим, що поперечна складова зовнішнього магнетного поля закриває спінонну щілину Δ_s у $SmMnO_{3+\delta}$. Характерною особливістю цього стану є просторове розділення зарядових і спінових збуджень. Згідно з цими дослідженнями, навіть слабке збільшення поперечної складової зовнішнього магнетного поля може привести до подальшого обмеження спінонних пар, що супроводжується появою безщілинних мод власних поздовжніх коливань системи спінового ланцюга. Ми припускаємо, що ступінчасті особливості польових залежностей намагнетованости $SmMnO_{3+\delta}$ за температури $T = 0{,}6$ К є подібними до характеристик ступінчастого квантового Голлового ефекту для безмасових Діракових ферміонів у графені.

Key words: quantum Luttinger liquid, 1*D* charge–spin density waves, confinement of spinon pairs, step-like quantum Hall effect for massless Dirac fermions.

Ключові слова: Латтинжерова квантова рідина, одновимірні хвилі зарядово-спінової густини, обмеження спінонних пар, ступінчастий квантовий Голлів ефект для безмасових Діракових ферміонів.

(Received 4 September, 2025)

1. INTRODUCTION

In Refs. [1, 2], a Luttinger exactly soluble model of a one-dimensional many-fermion system is discussed. The model has a fairly realistic interaction between pairs of fermions. An exact calculation of the momentum distribution in the ground state is given. As shown, there is no discontinuity in the momentum distribution in this model at the Fermi surface, but that the momentum distribution has infinite slope there. Comparison with the results of perturbation theory for the same model is also presented, and it is shown that, for this case at least, the perturbation and exact answers behave qualitatively alike. Finally, the response of the system to external fields is also discussed. As shown, he did not solve his model properly because of the paradoxical fact that the density operator commutators, which always vanish for any finite number of particles, no longer vanish in the field-theoretic limit of a filled Dirac sea. In fact, the operators define a boson field, which is *ipso facto* associated with the Fermi–Dirac field. This observation to solve the model was used and was obtained the exact (and now non-trivial) spectrum, free energy, and dielectric constant. This was also extended to interactions, which are more realistic. According to Ref. [3], one powerful approach to 1*D*-lattice fermion systems is to utilize a particular continuum limit to derive a low-energy effective model that can be solved analytically. For the simplest case of spinless fermions with local interactions away from half-filling, this approach leads to the so-called Luttinger model [1], which can be solved exactly using bosonization [2].

Exact solubility means a lot in this case: not only the partition function, but also all Green's functions of the Luttinger model can be computed exactly by analytical methods. This method can be generalized to 1D Hubbard-like systems and is the basis of a paradigm for 1D interacting fermion systems. In Ref. [3], a detailed derivation of a two dimensional (2D) low energy effective model for spinless fermions on a square lattice with local interactions is given. This derivation utilizes a particular continuum limit that is justified by physical arguments. It is shown that the effective model thus obtained can be treated by exact bosonization methods. It is also discussed how this effective model can be used to obtain physical information about the corresponding lattice fermion system.

According to Ref. [11], the problem of interacting fermions simplifies in one dimension. In a pioneering paper, Tomonaga treated the case of a two-body interaction, which is long ranged in real space. He showed that the low-energy excitations of the noninteracting as well as the interacting system can be described in terms of noninteracting bosons. The important idea to solve the case of interacting fermions was the observation that a long-range interaction in real space is short ranged in momentum space and therefore only particles and holes in the vicinity of the Fermi points are involved in the interacting ground state and states with low excitation energy. To obtain his results, Tomonaga linearized the energy dispersion around the two Fermi points $\pm k_F$. Luttinger later used a model with strictly linear energy dispersions, which is closely related to the massless Thirring's model. A very elegant method to calculate correlation functions for the model is the bosonization of the fermion field operator. The exponents of the anomalous power law decay of various correlation functions are determined by the anomalous dimension, which can be calculated explicitly for the Tomonaga–Luttinger (TL) model. It was an important observation of Haldane that the low-energy physics of the exactly solvable TL-model provides the generic scenario for one-dimensional fermions with repulsive interactions. Like in the Landau's Fermi-liquid picture, a few parameters completely determine the low energy physics.

Generally, they are as difficult to calculate as the Landau parameters. In contrast to the higher dimensional case, there are additional exactly solvable models, for which Haldane's Luttinger liquid scenario can be tested and the parameters determining the anomalous dimension can be calculated using the Bethe-ansatz technique. Another important manifestation of Luttinger liquids is called spin–charge separation, *i.e.*, for low energy excitations, the charge and spin degrees are completely decoupled. This shows up, for example, in the spectral function of the one-particle Green's function, which largely determines the photoemission spectrum. Recent high-resolution photoemission experiments on quasi-one-dimensional organic conductors have been interpreted to show Luttinger-liquid behaviour.

In Ref. [12], it was investigated the electronic band structure of Pt-induced nanowires on Ge(001) [Pt/Ge(001) NWs] by angle-resolved photoelectron spectroscopy at 6 K. Single-domain samples of Pt/Ge(001) NWs were prepared on vicinal Ge(001) substrates. One of the bands disperses only in the nanowire direction, and its Fermi surface consists of strictly straight lines, indicating that it is an ideal one-dimensional metallic state. An energy distribution curve of the one-dimensional band is explained by a Fermi–Dirac-type spectral shape, which is against both a Luttinger liquid and Peierls instability schemes. In Ref. [13], dispersing 1*D* bands have been observed for the first time in an organic conductor by high-resolution photoemission experiments on TTFTCNQ (tetrathiafulvalene tetracyanoquinodimethane). Their properties are extremely unusual: the bandwidth is much larger than traditional estimates, and the quasi-particle states are strongly renormalized, with no weight at the chemical potential. A deep pseudogap around the Fermi energy persists, and even increases, up to room temperature. Also was reported a direct determination of k_F in this material, and the observation of the opening of a Peierls gap in the low-temperature charge-density wave phase. In Ref. [14], it was presented that the Luttinger liquids are paramagnetic one-dimensional metals without Landau quasi-particle excitations. The elementary excitations are collective charge and spin modes, leading to charge–spin separation. Correlation functions exhibit power-law behaviour. All physical properties can be calculated, *e.g.*, by bosonization, and depend on three parameters only: the renormalized coupling constant K_ρ, and the charge and spin velocities.

Also it was discussed the stability of Luttinger liquids with respect to temperature, interchain coupling, lattice effects and phonons, and list important open problems. In Ref. [15], it was compute mean field phase diagrams of two closely related interacting fermion models in two spatial dimensions (2*D*). The first is the so-called 2*D* t–t'–V model describing spinless fermions on a square lattice with local hopping and density–density interactions. The second is the so-called 2*D* Luttinger model that provides an effective description of the 2*D* t–t'–V model, and in which parts of the fermion degrees of freedom are treated exactly by bosonization. In mean-field theory, both models have a charge-density-wave (CDW) instability making them gapped at half-filling. The 2*D* $t-t'-V$ model has a significant parameter regime away from half-filling, where neither the CDW nor the normal states are thermodynamically stable. It was shown that the 2*D* Luttinger model allows obtaining more detailed information about this mixed region. In this work, the confinement of low-energy thermal excitations of spinons in $SmMnO_{3+\delta}$ was found in the form of excitations of the type of nanofragments of 1*D* charge and spin-density waves, characteristic for low-energy excitations of a metallic one-dimensional quantum Luttinger liquid.

2. MATERIAL AND METHODS

Samples of self-doped manganites $SmMnO_{3+\delta}$ ($\delta \cong 0.1$) were obtained from high-purity oxides of lanthanum, samarium and electrolytic manganese, taken in a stoichiometric ratio. The synthesized powder was pressed under pressure of 10 kbar into discs of 6 mm in diameter, 1.2 mm thick and sintered in air at a temperature of 1170°C for 20 h followed by cooling at a rate of 70°C/h. The resulting tablets were a single-phase ceramic according to x-ray data. X-ray studies were carried out with 300 K on DRON-1.5 diffractometer in radiation Ni$K_{\alpha 1+\alpha 2}$. Symmetry and crystal lattice parameters were determined by the position and character splitting reflections of the perovskite-type pseudocubic lattice. Temperature and field dependences of dc magnetization were measured using a VSM EGG (Princeton Applied Research) vibrating magnetometer and a nonindustrial magnetometer in ZFC and FC modes. When measuring the temperature dependences of the magnetization $M(T)$ in the ZFC mode, the sample was first cooled to 4.2 K in a zero external magnetic field, followed by an increase in temperature to the required value. In the FC mode for measuring the magnetization $M(T)$, the sample was first cooled to 4.2 K in magnetic fields of various strengths, followed by heating. The field dependences of the magnetization $M(H)$ were measured during sample remagnetization at a temperature of 4.2 K in a wide range of magnetic fields in the ZFC and FC measurement modes.

3. EXPERIMENTAL RESULTS AND DISCUSSION

In this work, the field dependences of $SmMnO_{3+\delta}$ magnetization were investigated in the ZFC and FC measurement mode in the magnetic field range of ±5000 Oe (Figs. 1–4). The confinement of low-energy thermal excitations of spinons in $SmMnO_{3+\delta}$ was found in the form of excitations of the type of nanofragments of 1*D* charge and spin density waves, characteristic of low-energy excita-

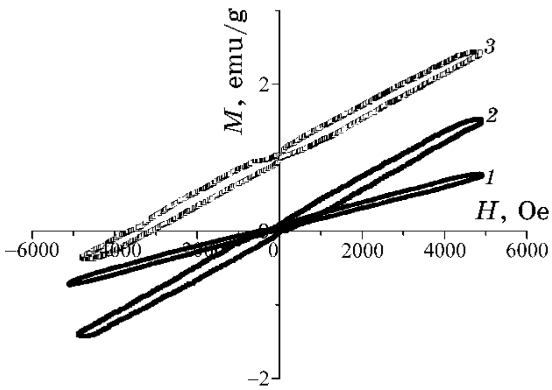

Fig. 1. Field dependences of magnetization of $SmMnO_{3+\delta}$ in the ZFC measurement mode in the form of isotherms of magnetization reversal of samples with different directions of growth of the external magnetic-field strength at $T = 0.6$ K (*1*) and $T = 4.2$ K (*2*). Field dependences of magnetization of $SmMnO_{3+\delta}$ at $T = 4.2$ K in the FC measurement mode (*3*).

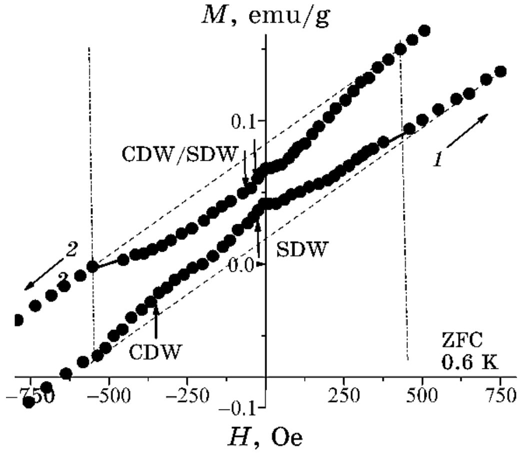

Fig. 2. Field dependences of magnetization of $SmMnO_{3+\delta}$ at $T = 0.6$ K in the ZFC measurement mode in the form of isotherms 1 and 2 of magnetization reversal of samples with different directions of growth of the external magnetic-field strength. As can be seen in this figure, during the magnetization reversal of the sample in the ZFC measurement mode, two peak features of magnetization are formed near $H = 0$ Oe in the range of magnetic fields of ±500 Oe.

tions of a metallic one-dimensional quantum Luttinger liquid.

With an increase in the external magnetic-field strength, a second-order quantum phase transition of the QSL to the Luttinger liquid state occurs, induced by an increase in the external magnetic-

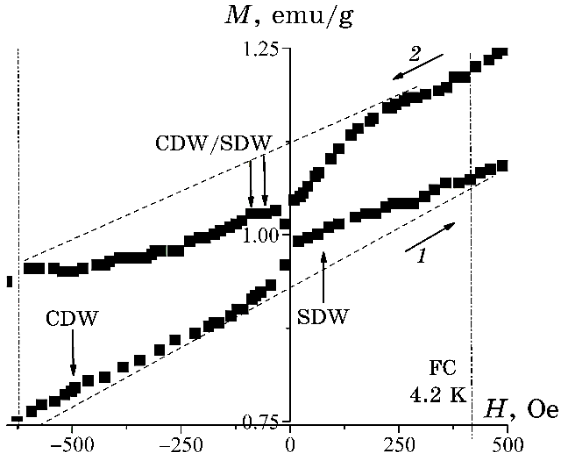

Fig. 3. Field dependences of magnetization of $SmMnO_{3+\delta}$ at $T = 4.2$ K in FC measurement mode in the form of isotherms 1 and 2 of magnetization reversal of samples with different directions of growth of the external magnetic-field strength. During the magnetization reversal of the sample in FC measurement mode, two peak features of magnetization are formed near $H = 0$ Oe in the magnetic-field range of ±500 Oe.

field strength. As a result of this transition, near $H = 0$ Oe, peak features of 'supermagnetization' are formed with varying degrees of their overlap, characteristic of the excitation of gapless decoupled charge and spin density waves in a Luttinger liquid. As can be seen in these figures, during the magnetization reversal in two measurement modes, two peak features of the magnetization $M(H)$ near $H = 0$ Oe are formed in the range of magnetic fields of ±500 Oe (Figs. 2, 3).

The difference between the two peak features of isotherms 1 and 2 of the magnetization reversal near $H = 0$ Oe, which depends on the direction of growth of the external magnetic-field strength, is noteworthy. As can be seen in Figs. 3 and 4, with an increase in the magnetic field in the positive direction (isotherm 1), separate CDW and SDW states are realized, which are not related to each other. At the same time, when the sign of the field growth changes to the opposite (isotherm 2), we observe near $H = 0$ Oe related CDW/SDW states that stimulates the transition of the system of zigzag AFM spin chains weakly coupled by the exchange interaction into a state similar to a metallic Luttinger liquid.

We believe that such behaviour of the magnetization in the low-temperature region is caused by the fact that the transverse component of the external magnetic field closes the spinon gap Δ_s for $SmMnO_{3+\delta}$. A characteristic feature of this state is the spatial sepa-

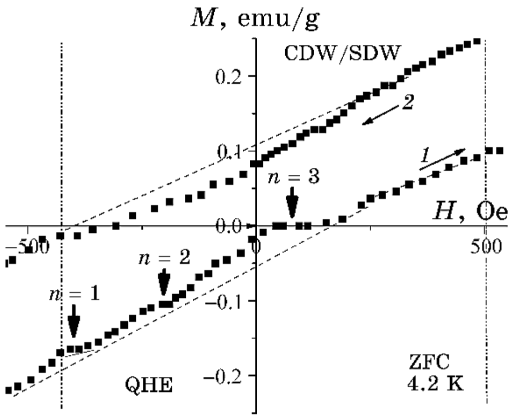

Fig. 4. Field dependences of magnetization of $SmMnO_{3+\delta}$ at $T = 4.2$ K in the ZFC measurement mode in the form of isotherms 1 and 2 of magnetization reversal of samples with different directions of growth of the external magnetic-field strength. As can be seen in the figure, during the magnetization growth of the sample in the ZFC measurement mode, three unusual step-like features of magnetization $M(H)$ are formed near $H = 0$ Oe that characteristic for forming of Landau bands in a Luttinger liquid. We explain the formation of a wide dip in magnetization near zero external magnetic field in isotherm 2 with the decay of the bound state of charge/spin density waves (CDW/SDW) during the process of sample demagnetization.

ration of charge and spin excitations. In this quasi-one-dimensional state, multiparticle excitations in the form of $1D$ charge and spin density waves, which obey the Bose statistics, dominate and largely replace elementary excitations in the form of spinon pairs. Of interest is the result that decoupled charge/spin density waves are formed in isotherms 1, whereas coupled $1D$ CDW/SDW collective excitation of the quantum spin liquid arises in isotherms 2 near zero magnetic field. Excitation of such $1D$ collective states in an external magnetic field was observed earlier in systems of weakly-coupled exchange Heisenberg and Ising AFM spin chains with different configurations and degrees of anisotropy. According to these studies, even a weak increase in the transverse component of the external magnetic field can lead to further confinement of spinon pairs, which is accompanied by the appearance of gapless modes of natural longitudinal oscillations of the spin chain system.

According to Ref. [6], in the limit of low excitation energies of a one-dimensional Mott dielectric, spin–charge separation occurs, which made it possible to accurately calculate their dynamic spectral function of charge density and spin $A(\omega, k_F + q)$. It was found that, in a one-dimensional Mott dielectric at a temperature $T = 0$ K, the excitation and annihilation operators of an ensemble of fermions with left and right directions of motion separate them into separate charge and spin regions as a result of bosonization in the form of fragments of separated one-dimensional charge density waves (CDW) and spin density waves incommensurate with the crystal lattice. We believe that the appearance of two unusual peak features of isotherms 1 and 2 of the magnetization reversal of $SmMnO_{3+\delta}$ near zero magnetic field are a natural consequence of the spin–charge separation characteristic of the previously well-studied theoretically one-dimensional Mott insulator in the state of a quantum Luttinger liquid [6, 7]. Attention is drawn to the difference between the two peak features of isotherms 1 and 2 of the magnetization reversal near $H = 0$ Oe, which depends on the direction of growth of the external magnetic-field strength. As can be seen in Figs. 2, 3, with the increase of the magnetic field in the positive direction (isotherm 1), separate CDW and SDW states are realized, which are not related to each other. At the same time, when the sign of the field growth changes to the opposite (isotherm 2), we observe near $H = 0$ Oe the CDW/SDW states related to each other that stimulates the transition of the system of zigzag AFM spin chains weakly coupled by the exchange interaction to a state similar to the metallic Luttinger liquid. We believe that such behaviour of magnetization in the low-temperature region is caused by the fact that the transverse component of the external magnetic field closes the spinon gap Δ_s for $SmMnO_{3+\delta}$. A characteristic feature of this state is the spatial separation of charge and spin excitations.

In this quasi-one-dimensional state, multiparticle excitations in the form of 1D charge and spin density waves, which obey the Bose statistics, dominate and largely replace elementary excitations in the form of spinon pairs. Of interest is the result that decoupled charge/spin density waves are formed in isotherms 1, whereas coupled 1D CDW/SDW collective excitation of the quantum spin liquid arises in isotherms 2 near zero magnetic field. Excitation of such 1D collective states in an external magnetic field was observed earlier in systems of weakly-coupled exchange Heisenberg and Ising AFM spin chains with different configurations and degrees of anisotropy. According to these studies, even a weak increase in the transverse component of the external magnetic field can lead to further confinement of spinon pairs, which is accompanied by the appearance of gapless modes of natural longitudinal oscillations of the spin chain system.

Field dependences of magnetization $M(H)$ of $SmMnO_{3+\delta}$ at $T = 4.2$ K in the ZFC measurement mode (Fig. 4) differ greatly from the graphs presented in Figs. 2, 3. As can be seen in these figures, during the magnetization of the sample in the ZFC measurement mode, three step-like features of magnetization are formed near $H = 0$ Oe in the range of magnetic fields of ± 500 Oe (isotherm 1). During the process of demagnetization of the sample (isotherm 2) in the magnetic-field range of ± 500 Oe, a wide dip is formed with an extreme drop in the magnetization of the sample $M(H)$ near the zero field. We explain the formation of a wide dip in magnetization near zero external magnetic field in isotherm 2 with the decay of the bound state of charge/spin density waves (CDW/SDW) during the process of sample demagnetization.

We assume that step-like features of field dependences of magnetization of $SmMnO_{3+\delta}$ (Fig. 4) are similar characteristic of quantum Hall effect for massless Dirac fermions in graphene [16–18]. In Ref. [16], it first was reported a condensed matter system, where electron transport is essentially governed by the Dirac equation and charge carriers mimic relativistic particles with zero mass and an effective 'speed of light' $c^* \approx 10^6$ m/s. The unusual response of massless fermions to magnetic field is highlighted further by their behaviour in the high-field limit, where there is the quantum Hall effect (QHE). It was shown the Hall conductivity σ_{xy} of graphene plotted as a function of electron and hole concentrations in a constant field **B**. Pronounced QHE plateaux are clearly seen but, surprisingly, they do not occur in the expected sequence $\sigma_{xy} = (4e^2/h)N$, where N is integer. On the contrary, the plateaux correspond to half-integer ν, so that the first plateau occurs at $2e^2/h$ and the sequence is $(4e^2/h)(N + 1/2)$. Note that the transition from the lowest hole ($\nu\ \ -1/2$) to lowest electron ($\nu = +1/2$) Landau level (LL) in graphene requires the same number of carriers ($\Delta n = 4B/\varphi_0 \approx 1.2 \cdot 10^{12}$ cm^{-2}) as the transition between other nearest levels (cf. distances between minima in ρ_{xx}).

This one results in a ladder of equidistant steps in σ_{xy}, which are not interrupted, when passing through zero. To emphasize this highly unusual behaviour, it was shown that σ_{xy} for a graphite film consisting of only two graphene layers, where the sequence of plateaux returns to normal and the first plateau is at $4e^2/h$, as in the conventional QHE. It was attributed this qualitative transition between graphene and its two-layer counterpart to the fact that fermions in the latter exhibit a finite mass near $n \cong 0$ (as found experimentally and to be published elsewhere) and can no longer be described as massless Dirac particles. These studies of graphene have revealed a variety of unusual phenomena characteristic of two-dimensional ($2D$) Dirac fermions. In particular, it was observed that: a) the integer quantum Hall effect in graphene is anomalous in that it occurs at half-integer filling factors; b) graphene conductivity never falls below a minimum value corresponding to the conductance quantum e^2/h, even when carrier concentrations tend to zero; c) the cyclotron mass m_c of massless carriers with energy E in graphene is described by equation $E = m_c c_*^2$; d) Shubnikov–de Haas oscillations in graphene exhibit a phase shift of π due to Berry's phase. As can be seen in Fig. 4 in this work, during the magnetization growth of the sample in the ZFC measurement mode, three step-like features of magnetization $M(H)$ are formed near $H = 0$ Oe that is characteristic for forming three Landau bands in a Luttinger liquid.

According to Ref. [17], when electrons are confined in two-dimensional (2D) materials, quantum-mechanically enhanced transport phenomena, as exemplified by the quantum Hall effect, can be observed. Graphene, an isolated single atomic layer of graphite, is an ideal realization of such a 2D system. The low-energy band structure of graphene can be approximated as cones located at two inequivalent Brillouin-zone corners. In these cones, the 2D energy dispersion relation is linear and the electron dynamics can be treated as 'relativistic,' where the Fermi velocity v_F of the graphene plays the role of the speed of light. In particular, at the apex of the cones (termed Dirac point), electrons and holes (particles and antiparticles) are degenerate. Landau level (LL) formation for electrons in such a system under a perpendicular magnetic field, **B**, has been studied theoretically using an analogy to the $2 + 1$ dimensional quantum electrodynamics. The exceptionally high-mobility graphene samples allow investigating transport phenomena in the extreme magnetic quantum limit, such as the QHE. In this work, the overall positive R_{xy} indicates that the contribution is mainly from electrons. At high external magnetic fields $B \cong 1–8$ T, $R_{xy}(B)$ exhibits step-like features (plateaus), and R_{xx} is vanishing, which are the hallmark of the QHE. At least two well-defined plateaus are observed before the QHE features transform into Shubnikov–de Haas oscillations at lower magnetic field. The quantization of R_{xy} for these first two plateaus is better than 1 part in 10^4, precise within the instrumental uncertainty.

In Ref. [18], the quantum Hall effect with a Berry's phase of π is demonstrated on a single graphene layer grown on the C-face of 4H silicon carbide. The mobility is of $\cong 20000$ cm^2/(V·s) at 4 K and 15000 cm^2/(V·s) at 300 K despite contamination and substrate steps. This is comparable to the best-exfoliated graphene flakes on SiO_2 and an order of magnitude larger than Si-face epitaxial graphene monolayers. The QHE is well resolved in this sample, which shows quantum Hall plateaus in the magnetic-field dependence of the Hall resistance, as first observed in exfoliated graphene flakes on SiO_2. The Hall plateaus correspond to transverse resistances $\rho_{xy} = (h/4e^2)/(n + 1/2)$ for $n = 0$ to 3, where n is the Landau level index, which establishes the nontrivial Berry's phase of π. The longitudinal resistivity ρ_{xx} shows the characteristic Shubnikov–de Haas (SdH) oscillations (SdHOs), in which Landau levels from $n = 0$ up to $n = 8$ are easily recognized. The SdHOs develop into the QHE in high fields, manifested by characteristic zero resistance minima and Hall plateaus.

According to Ref. [19], the electronic properties of a graphite monolayer have attracted theoretical interest due to a Dirac-type spectrum of charge carriers in this gapless semiconductor. Recently, Novoselov *et al.* fabricated ultra-thin graphitic devices including monolayer structures. This was followed by further observations of the classical and quantum Hall effects in such systems confirming the expectations of an unusual phase of Shubnikov–de Haas oscillations and QHE plateaus sequencing, as manifestations of a peculiar magneto-spectrum of chiral Dirac-type quasi-particles containing a Landau level at zero energy. In Ref. [19], it was studied an effective two-dimensional Hamiltonian to describe the low-energy electronic excitations of a graphite bilayer, which correspond to chiral quasi-particles with a parabolic dispersion exhibiting Berry's phase of 2π. Its high-magnetic-field Landau level spectrum consists of almost equidistant groups of four-fold degenerate states at finite energy and eight zero-energy states. This can be translated into the Hall conductivity dependence on carrier density, $\sigma_{xy}(N)$, which exhibits plateaus at integer values of $4e^2/h$ and has a 'double' $8e^2/h$ step between the hole and electron gases across zero density, in contrast to $(4n + 2)e^2/h$ sequencing in a monolayer.

According to Ref. [20], the half-integer quantum Hall effect in single-layer graphene (SLG) 1, 2 and the unconventional quantum Hall effect in bilayer graphene (BLG) 3 reveal spin- and valley-degenerate relativistic Landau levels. Due to the extremely large Landau-level splitting, completely-resolved levels can be observed up to room temperature. However, even at very high perpendicular magnetic fields, the Zeeman splitting within one Landau level is negligible smaller compared to the Landau-level splitting and, more importantly, the Landau-level width generally exceeds the spin splitting. Exceptionally, the zeroth Landau level in SLG becomes extremely narrow at magnetic fields $B > 20$ T that allows an experimental observation of a spin-related gap opening at magnetic fields $B > 20$ T. Another observation of a spin degeneracy lifting with an effective g factor $g^* = 2$ was reported for $\nu = \pm 4$ in SLG for magnetic fields $B > 30$ T, combined with lifting the valley degeneracy at $\nu = \pm 1$. In Ref. [20], it was determined the spin splitting of broadened Landau levels for SLG and BLG by measuring SdH oscillations in tilted magnetic fields. This technique allows adjusting the ratio between the spin splitting and the Landau-level splitting by controlling the ratio between a total magnetic field and a component perpendicular to a two-dimensional graphene flake. Using the well-established Lifshitz–Kosevich formula, it was determined the product of the effective g factor and cyclotron mass m^*g^* from the angular dependence of the SdH amplitudes, and it was found that g^* is enhanced compared to the free-electron value.

Similar stepwise oscillations of magnetization were previously discovered by us for $SmMnO_{3+\delta}$ in the temperature dependences of $M(T)$ [21]. According to Ref. [21], quantum oscillations of the temperature dependence $M(T)$ of the magnetization of $SmMnO_{3+\delta}$ (QHE) measured in the strong magnetic field $H = 3.5$ kOe in the temperature range 4.2–12 K have an unusual form. With an increase in the field to $H = 3.5$ kOe, a step-like quantization of the spinon spectrum appeared in the form of the formation of threshold features of magnetization in the Landau bands $n = 1$, $n = 2$, and $n = 3$ in the kind of steps (plateaus) corresponding to the integer filling of three Landau bands with a finite gap by spinons. As the temperature rises, the height of the thresholds and the width of the steps increase. Emergence of new quantum oscillations of the magnetization temperature dependences in the strong field regime of measurements is caused by the Landau quantization by the gauge field of the spinon gas with a fractional spin $S = 1/2$, moving on circular orbits in the direction transverse to the direction of the 'magnetic' component B of the gauge field.

4. CONCLUSIONS

According to the theory, in the limit of low excitation energies of a one-dimensional Mott dielectric, spin–charge separation occurs, which made it possible to accurately calculate their dynamic spectral function of charge density and spin $A(\omega, k_F+q)$. It was found that in a one-dimensional Mott dielectric at a temperature $T = 0$ K, the excitation and annihilation operators of an ensemble of fermions with left and right directions of motion separate them into separate charge and spin regions as a result of bosonization in the form of fragments of separated one-dimensional charge density waves (CDW) and spin density waves incommensurate with the crystal lattice. We believe that the appearance of two unusual peak features of isotherms 1 and 2 of the magnetization reversal of $SmMnO_{3+\delta}$ near zero magnetic field are a natural consequence of the spin–charge separation characteristic of a quantum Luttinger liquid. Attention is drawn to the difference between the two peak features of isotherms 1 and 2 of the magnetization reversal near $H = 0$ Oe, which depends on the direction of growth of the external magnetic-field strength. As can be seen in Figs. 2, 3, with the increase of the magnetic field in the positive direction (isotherm 1) separate

CDW and SDW states are realized, which are not related to each other. At the same time, when the sign of the field growth changes to the opposite (isotherm 2), we observe near $H = 0$ Oe the CDW/SDW states related to each other that stimulates the transition of the system of zigzag AFM spin chains weakly coupled by the exchange interaction to a state similar to the metallic Luttinger liquid. We believe that such behaviour of magnetization in the low-temperature region is caused by the fact that the transverse component of the external magnetic field closes the spinon gap Δ_s in $SmMnO_{3+\delta}$. A characteristic feature of this state is the spatial separation of charge and spin excitations.

In this quasi-one-dimensional state, multiparticle excitations in the form of $1D$ charge and spin density waves, which obey the Bose statistics, dominate and largely replace elementary excitations in the form of spinon pairs. Of interest is the result that decoupled charge/spin density waves are formed in isotherms 1, whereas coupled $1D$ CDW/SDW collective excitation of the quantum spin liquid arises in isotherms 2 near zero magnetic field. Excitation of such $1D$ collective states in an external magnetic field was observed earlier in systems of weakly-coupled exchange Heisenberg and Ising AFM spin chains with different configurations and degrees of anisotropy. According to these studies, even a weak increase in the transverse component of the external magnetic field can lead to further confinement of spinon pairs, which is accompanied by the appearance of gapless modes of natural longitudinal oscillations of the spin chain system.

We assume that step-like features of field dependences of magnetization of $SmMnO_{3+\delta}$ at temperature $T = 0.6$ K are similar characteristic of quantum Hall effect for massless Dirac fermions in graphene. In these works, it was firstly observed a condensed matter system, where electron transport is essentially governed by the Dirac equation and charge carriers mimic relativistic particles with zero mass and an effective ‘speed of light’ $c^* \cong 10^6$ m/s. These studies of graphene have revealed a variety of unusual phenomena characteristic of two-dimensional ($2D$) Dirac fermions. In particular, it was observed that: a) the step-like quantum Hall effect in graphene is anomalous in that it occurs at half-integer filling factors; b) graphene conductivity never falls below a minimum value corresponding to the conductance quantum e^2/h, even when carrier concentrations tend to zero; c) the cyclotron mass m_c of massless carriers with energy E in graphene is described by equation $E = m_c c^{*2}$; d) Shubnikov–de Haas oscillations in graphene exhibit a phase shift of π due to Berry’s phase. During the magnetization growth of the sample in the ZFC measurement mode, three step-like features of magnetization $M(H)$ are formed near $H = 0$ Oe that is characteristic for forming three Landau bands in a Luttinger liquid.

The low-energy band structure of graphene can be approximated as cones located at two inequivalent Brillouin-zone corners. In these cones, the 2*D* energy dispersion relation is linear and the electron dynamics can be treated as 'relativistic', where the Fermi velocity v_F of the graphene plays the role of the speed of light. In particular, at the apex of the cones (termed Dirac point), electrons and holes (particles and antiparticles) are degenerate. Landau level (LL) formation for electrons in such system under a perpendicular magnetic field, **B**, has been studied theoretically using an analogy to the $2+1$ dimensional quantum electrodynamics. The exceptionally high-mobility graphene samples allow investigating transport phenomena in the extreme magnetic quantum limit, such as the QHE. It was shown the overall positive R_{xy} that indicates the contribution from electrons mainly. At high external magnetic fields $B \cong 1-8$ T, $R_{xy}(B)$ exhibits step-like features (plateaus), and R_{xx} is vanishing, which are the hallmark of the QHE. At least two well-defined plateaus are observed before the QHE features transform into Shubnikov–de Haas oscillations at lower magnetic field. The quantization of R_{xy} for these first two plateaus is better than 1 part in 10^4, precise within the instrumental uncertainty.

REFERENCES

1. J. M. Luttinger, *J. Math. Phys.*, **4**: 1154 (1963); https://doi.org/10.1063/1.1704046
2. D. C. Mattis and E. H. Lieb, *J. Math. Phys.*, **6**: 304 (1965); doi:10.1063/1.1704281
3. E. Langmann, *arXiv:0903.0055v3 [math-ph]* 14 Apr 2010.
4. U. Ledermann, A dissertation submitted to the ETH Zürich for the degree of the Doctor of Natural Sciences (2001).
5. E. Langmann, *arXiv:math-ph/0606041v3* 14 Apr 2010.
6. J. Voit, *arXiv:cond-mat/9510014v1* 29 Sep 1995.
7. F. D. M. Haldane, *J. Phys. C*, **14**: 2585 (1981); doi:10.1088/0022-3719/14/19/010
8. J.-S. Caux and C. M. Smith, *arXiv:1702.03735v1 [cond-mat.str-el]* 13 Feb 2017.
9. J. Liang and J. Hu, *Quantum Frontiers*, **4**: 1 (2025); https://doi.org/10.3389/fphy.2025.1541888
10. S. Rao and D. Sen, *arXiv:cond-mat/0005492v2* 6 Jul 2001.
11. K. Schönhammer and V. Meden, *arXiv:cond-mat/9606018v1* 5 Jun 1996.
12. K. Yaji, I. Mochizuki, S. Kim, Y. Takeichi, A. Harasawa, Y. Ohtsubo, P. Le Fèvre, F. Bertran, A. Taleb-Ibrahimi, A. Kakizaki, and F. Komori, *Phys. Rev. B*, **87**: 241413(R) (2013); https://doi.org/10.1103/PhysRevB.87.241413
13. F. Zwick, D. Jérome, G. Margaritondo, M. Onellion, J. Voit, and M. Grioni, *Phys. Rev. Lett.*, **81**: 2974 (1998);

https://doi.org/10.1103/PhysRevLett.81.2974
14. J. Voit, *arXiv:cond-mat/0005114v1 [cond-mat.str-el]* 5 May 2000.
15. J. de Woul and E. Langmann, *arXiv:0907.1277v2 [math-ph]* 16 Apr 2010.
16. K. S. Novoselov, A. K. Geim, S. V. Morozov, D. Jiang, M. I. Katsnelson, I. V. Grigorieva, S. V. Dubonos, and A. A. Firsov, *Nature (London)*, **438**: 197 (2005); https://doi.org/10.1038/nature04233438
17. Y. Zhang, Y.-W. Tan, H. Stormer, and P. Kim, *Nature (London)*, **438**: 201 (2005); https://doi.org/10.1038/nature04235
18. X. Wu, Y. Hu, M. Ruan, N. K. Madiomanana, J. H. Hankinson, M. Sprinkle, C. Berger, and W. A. de Heer, *Applied Physics Letters*, **95**, No. 22: 223108 (2009); doi:10.1063/1.3266524. hal-01002933
19. E. McCann and V. I. Fal'ko, *arXiv:cond-mat/0510237v2 [cond-mat.mes-hall]* 3 Mar 2006.
20. E. V. Kurganova, H. J. van Elferen, A. McCollam, L. A. Ponomarenko, K. S. Novoselov, A. Veligura, B. J. van Wees, J. C. Maan, and U. Zeitler, *Phys. Rev. B*, **84**: 121407(R) (2011); doi:10.1103/PhysRevB.84.121407
21. F. N. Bukhanko and A. F. Bukhanko, *Low Temp. Phys.*, **47**: 937 (2021); https://doi.org/10.1063/10.0006569